ACS OMEGA

http://pubs.acs.org/journal/acsodf

Article

Coaxial Electrospun Nanofibers with Different Shell Contents to Control Cell Adhesion and Viability

Jae Keun Park,[§] Oanh-Vu Pham-Nguyen,[§] and Hyuk Sang Yoo*

Cite This: *ACS Omega* 2020, 5, 28178−28185

Read Online

ACCESS | Metrics & More | Article Recommendations | Supporting Information

ABSTRACT: Electrospun nanofibers are widely employed as cell culture matrices because their biomimetic structures resemble a natural extracellular matrix. However, due to the limited cell infiltration into nanofibers, three-dimensional (3D) construction of a cell matrix is not easily accomplished. In this study, we developed a method for the partial digestion of a nanofiber into fragmented nanofibers composed of gelatin and polycaprolactone (PCL). The PCL shells of the coaxial fragments were subsequently removed with different concentrations of chloroform to control the remaining PCL on the shell. The swelling and exposure of the gelatin core were manipulated by the remaining PCL shells. When cells were cultivated with the fragmented nanofibers, they were spontaneously assembled on the cell sheets. The cell adhesion and proliferation were significantly affected by the amount of PCL shells on the fragmented nanofibers.

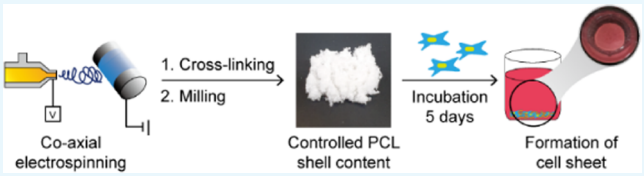

1. INTRODUCTION

In tissue engineering, a scaffold provides mechanical support and a microenvironment to promote cell growth and tissue regeneration.[1] The structure of a biomimetic scaffold resembles a native extracellular matrix (ECM). An ECM is formed by an arrangement of nanofibers with diameters ranging from 50 to 500 nm[2] and consists of collagen, elastin, fibronectin, and proteoglycan,[3,4] which make up the base layer. An ideal cell scaffold is similar to a native ECM and provides a three-dimensional (3D) environment to support cell attachment, proliferation, and maturity. A 3D scaffold provides another direction for cell−cell interaction, cell movement, and cell morphology formation.[5] There are different ways to develop 3D fibrous scaffolds capable of providing these 3D environments. One method is based on the microembossing technology. For example, a bilayer-embossing 3D scaffold was developed using poly(DL-lactide-*co*-glycolide) and poly(dimethylsiloxane) (PDMS) molds to create a well-defined 3D tissue engineering scaffold.[6] The cell grown in the developed scaffold showed fine strands and was observed to spread in three dimensions. Another method is based on 3D printing technology. In one study, a 3D-printed porous gelatin methacrylamide structure was developed to achieve high cell viability.[7] The 3D-printed scaffold had controlled pore sizes, stable mechanical strength, and high cell viability.

Electrospinning has been widely used to prepare biomimetic scaffolds resembling a fibrous ECM. Nanofibrous structures such as nanofiber mats can be easily prepared using electrospinning.[8,9] These mats are used as 3D fibrous scaffolds because they have a large surface area[10,11] as well as porosity[12] and are known to have a structure that mimics an ECM. Among various biocompatible polymers that are suitable for 3D scaffolds, polycaprolactone (PCL) has been successfully used in tissue engineering. PCL nanofibers prepared for cartilage tissue engineering showed a higher level of mesenchymal stem cell chondrogenesis than cell pellet culture.[13] In addition, aligned PCL nanofibers collected from rotating drums were used in neurotissue engineering, and this facilitated neurite infiltration, while did not cause any immune response.[14] PCL/gelatin composite nanofibers developed for muscle tissue engineering were electrospun using a mixture of PCL and gelatin, and the PCL/gelatin nanofibers (GNFs) showed better formation of myotubes than the pure PCL nanofibers.[15] For nerve regeneration, the PCL/collagen nanofiber was prepared by electrospinning a solution of PCL and collagen in a 1/1 weight ratio on a rotational drum composed of a stainless steel rod having a small diameter.[16] These studies showed that the PCL nanofibers provided higher cell adhesion because of the hydrophobicity of PCL. However, a high hydrophobicity prevents cell migration in the perpendicular direction to fibrous meshes. In addition, the long-term viability of the cultivating cells could not be considerably enhanced because hydrophobic polymers become swollen easily unlike polymeric hydrogels.

Electrospinning of gelatin is a challenging task because gelatin is a water-soluble polymer. Owing to the limited evaporation during the electrospinning process, water-based electrospinning is difficult because the charged jets from the

Received: August 13, 2020
Accepted: October 9, 2020
Published: October 22, 2020

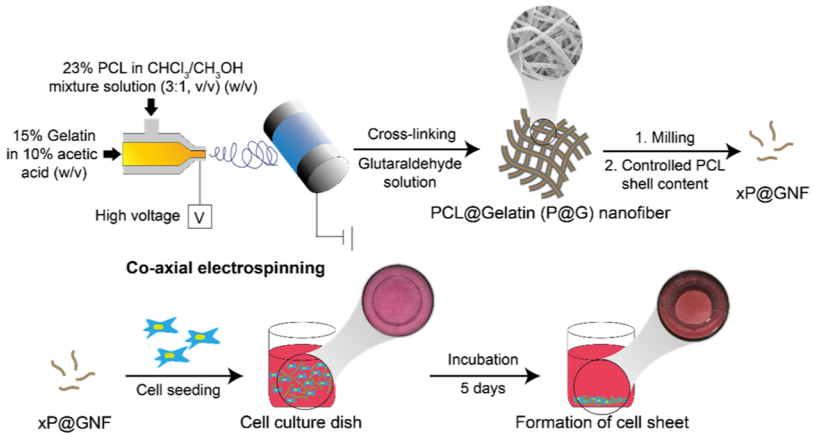

Figure 1. Schematic diagram for preparation of gelatin nanofibrils (GNFs) with various amounts of PCL shells and cell sheet formation with the engineered GNF. A coaxial nozzle was employed to fabricate core−shell nanofibers composed of PCL and gelatin, which were subsequently cross-linked with glutaraldehyde (P@G nanofibers). P@G nanofibers were milled and treated with a mixture of chloroform/ethanol to fabricate gelatin nanofibrils with a partial PCL shell (*x*P@GNF, *x* = (remaining PCL/initial PCL (%, w/w))). Cells were seeded with *x*P@GNF to form cell sheets for 5 days.

ejection needles are not separated to form a nanofibrous morphology. Therefore, water-soluble polymers are generally blended with poly(vinyl alcohol) (PVA) or poly(ethylene oxide) for better electrospinnability. To overcome this issue, we performed coaxial electrospinning with an inner and an outer needle so that the two immiscible solvents could be coejected and electrospun to form fibrous meshes.[17,18] In our previous study, we employed PCL as a sacrificial layer to maintain a fibrous morphology until the gelatin inner core was fully cross-linked with glutaraldehyde (GTA). We observed that the fibrous morphology was well maintained during the process and confirmed the viscoelastic properties of the cross-linked gelatin in the nanofibers. However, previous studies were limited by the slow cell migration into the fibrous meshes resulting from the nanoporous structures of the nanofibers. We also investigated fragmented fibrils composed of semi-hydrolyzed nanofibers to facilitate cell migration during cell proliferation.[19] When surface-functionalized PCL nanofibers were fragmented in an optimized condition, the fragmented fibrils exhibited features that were significantly different from that of nanofibrous meshes in terms of cell attachment, migration, and proliferation.[20] Seeded cells were self-assembled into cell sheets with the fibrils in several ways according to the ratio between the cells and the matrix.[21] These cell sheets could be directly transferred to many defect sites, including de-epithelized wound sites, osteochondral defect sites, and myogenic defect sites.[22,23]

In the present study, we electrospun fibrous meshes with a coaxial nozzle to coeject the gelatin core and the PCL shell, and the gelatin core was cross-linked for further fragmentation into nanofibrils. After the conditioned etching of PCL shells of the nanofibrils with an organic solvent, PCL/gelatin nanofibrils with different PCL contents in the fibrils were obtained. Previous reports indicated that a hydrophobic surface such as PCL can be a good substrate for cell adhesion at the initial stage of cell adhesion and nanofibrous scaffolds significantly enhanced cell spreading and elongation in comparison to microfibrous scaffolds.[24,25] Thus, we hypothesize that different covering degrees of the gelatin core with PCL can be used to manipulate cell adhesion, migration, and proliferation in the nanofibril matrix.

2. RESULTS AND DISCUSSION

We previously prepared hydronanofibrous meshes by two different strategies: (1) a bottom-up strategy of decorating surfaces after electrospinning and (2) a top-down strategy of eroding surfaces to obtain required surface properties after electrospinning. The "bottom-up" strategy was employed to deposit gelatin on the surfaces of nanofibers to obtain a high degree of cell viability,[18,22] "top-down" approach was employed for alginate nanofibrous meshes where the core alginate of the PCL/alginate coaxial nanofiber was cross-linked and the PCL shell was discarded.[17] Thus, we herein investigated the "top-down" strategy of gelatin nanofibers using PCL/gelatin coelectrospinning. In the current study, gelatin nanofibrils with different PCL shell contents were fabricated so that they can be tailored for optimized cell adhesion and proliferation to form self-assembled cell sheets, which could not be accomplished in previous studies. Herein, we combined our previous strategy of coaxial electrospinning PCL (shell) and gelatin (core)[26] with a simple method that involves the surface etching of coaxial nanofibrils through a solvent treatment to obtain gelatin nanofibrils with different amounts of PCL shells (Figure 1). Gelatin has been reported to be difficult to be electrospun because of its highly electrolytic properties.[12,26] Furthermore, when gelatin nanofibers are directly exposed to an aqueous phase, the fibrous morphology of the fibers may be deformed. Therefore, we prepared nanofibers with a core−shell structure of gelatin (core) surrounded by PCL (shell) through coaxial electrospinning and then cross-linked the core with GTA (P@G nanofiber). Previous reports have indicated that when a nanofiber mesh with nanoscale pore size was employed for cell cultivation, infiltration into the interior of the mesh was limited, and therefore the cells proliferated only on a horizontal surface in the 3D structure.[27] Therefore, the nanofibers (P@GNF) were further fragmented into nanofibrils to improve the cell−matrix interaction.[28] Additionally, we used a chloroform/MeOH mixture to control the amount of PCL shells on the nanofibrils (*x*P@GNF). A previous study showed that cell/nanofibril complexes exhibit hydrogel-like properties.[4] Therefore, a self-assembled cell sheet was obtained by incubating NIH3T3 cells with a controlled shell thickness for P@GNF (*x*P@GNF).

https://dx.doi.org/10.1021/acsomega.0c03902
ACS Omega 2020, 5, 28178−28185

The morphology of the P@G nanofibers and the changes in the diameter of the nanofibers were first investigated using a scanning electron microscope (SEM) (Figure S1). Multiple PCL flow rates were utilized to fabricate the P@G nanofibers, namely, 0.6, 1.2, and 1.5 mL/h. According to the SEM images, the PCL flow rate did not have a significant influence on the morphology and formation of P@G nanofibers (Figure S1a). However, the diameter of the nanofibers increased when the PCL flow rate was increased (Figure S1b). The diameters of the P@G nanofibers were 463 ± 79.2, 510.3 ± 68.6, and 570.3 ± 69.5 nm when the PCL flow rates were 0.6, 1.2, and 1.5 mL/h, respectively. To facilitate the surface-etching process of P@G nanofibers, we decided to fix the PCL flow rate at 1.5 mL/h for the rest of the study. On the other hand, we previously examined the morphology of the PCL nanofibrils.[18,22,29] After the solvent treatment, the PCL shell was supposed to be thinner. However, as we examined the core−shell structure of coaxial electrospun nanofibers in our previous study using a transmission electron microscope (TEM),[30] the PCL shell itself was confirmed to be very thin (<5 nm). It should be mentioned that the gelatin core can be highly swollen in an aqueous phase in comparison to PCL, and for TEM analysis, the nanofibrils should be freeze-dried where the ice phase in the frozen sample is evaporated. This may cause a superporous structure of the gelatin core, and the density of the core can be much lower than that of PCL. Therefore, we speculated that the change in shell thickness was not significant, and the morphology of P@GNF was retained after the solvent treatment. As a result, we speculated that the cell proliferation and attachment were mostly affected by the remaining PCL shell and exposure of the gelatin core.

The surface etching of P@G nanofibers was performed by treating the P@G nanofibers with a chloroform/MeOH mixture. The gelatin core was predicted to be exposed after the solvent treatment. Therefore, fluorescein isothiocyanate (FITC)-labeled gelatin was used for electrospinning to visualize the amount of exposed gelatin after the treatment with the solvent mixture. The electrospun nanofibers were treated with various volume ratios of chloroform/MeOH (0/10, 1/9, and 3/7) to obtain different contents of the remaining PCL shell (100P@GNF, 80P@GNF, and 50P@GNF, respectively). Then, the treated nanofibers were observed under a fluorescence microscope (Figure 2). As shown in the fluorescence microscopic images, the fluorescence intensity of FITC-gelatin increased as the nanofiber PCL content decreased. In addition, the microscopic images indicate that the surface-etching process did not have a significant effect on the morphology of the nanofibers. These results indicate that the gelatin core was successfully exposed to the surface due to the thinning of the PCL shell during the solvent treatment, while the shape of the nanofibers was retained. Multiple efforts have been made to solve the problems faced while electrospinning gelatin.[15,31] The most common solution is to mix gelatin with another polymer such as PCL. However, when the concentration of gelatin is increased, nanofibers are either not formed or do not have a constant diameter.[31] Meanwhile, the nanofibers fabricated using our method could help gelatin to be electrospun and guaranteed the integrity of gelatin at the nanofiber core.

In a previous study, core/shell nanofiber scaffolds containing PCL (shell) and alginate (core) were fabricated.[17] It was confirmed that alginate nanofibers were obtained by completely etching the PCL shell with chloroform while the shape of the nanofibers was retained. Therefore, we speculate that the contents of the remaining PCL shell can be controlled by adjusting the volume ratio of chloroform and MeOH. The remaining PCL shell is determined by calculating the changes in the weight of P@GNF before and after treatment with different solvents (Table 1). After P@GNF was treated with chloroform/MeOH (volume ratios of 0/10, 1/9, 3/7, and 5/5), the weight of the surface-etched P@GNF became 98.80 ± 0.95, 85.39 ± 2.01, 54.80 ± 1.02, and 10.30 ± 0.53 mg, respectively. On the other hand, the theoretical amount of the remaining PCL was calculated as follows. The concentration and flow rate of PCL/gelatin used for electrospinning were 0.23/0.15 g/mL and 1.5/0.3 mL/h, respectively. The nanofibers were collected every 30 min. The theoretical PCL weight was 0.23 g/mL × 1.5 mL/h × 0.5 h = 0.1725 g, and the theoretical gelatin weight was 0.15 g/mL × 0.3 mL/h × 0.5 h = 0.0225 g. Because PCL and gelatin were simultaneously located during the coaxial electrospinning process, the

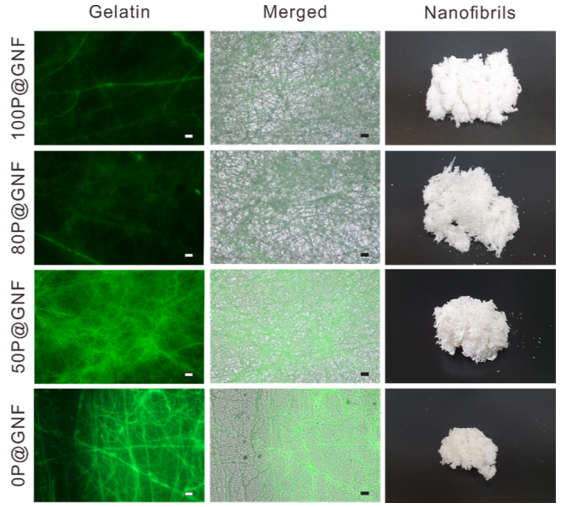

Figure 2. Fluorescence microscopic images of a gelatin nanofiber (GNF) with different PCL shell contents. Gelatin was fluorescently labeled with FITC and electrospun to nanofibers. Surface-etched nanofibers with different contents of PCL (100P@G nanofiber, 80P@G nanofiber, 50P@G nanofiber, 0P@G nanofiber) were observed for fluorescently labeled gelatin (Gelatin), overlapped images with light microscopic images (Merged), and digital images of 100P@GNF, 80P@GNF, 50P@GNF, and 0P@GNF (10 mg) after milling of the nanofibers (scale bar = 10 μm).

Table 1. Characterization of PCL Loss of P@GNF after Dissolving PCL in the Chloroform/MeOH (v/v) Mixture with Various Blending Ratios

*x*P@GNF	chloroform/MeOH (v/v)	weight before surface-etching (mg)	weight after surface-etching (mg)[a]	remaining weight of PCL in nanofibril (%)[b]
100P@GNF	0/10	100	98.80 ± 0.95	98.23 ± 0.82
80P@GNF	1/9		85.39 ± 2.01	84.00 ± 3.03
50P@GNF	3/7		54.80 ± 1.02	49.71 ± 2.39
0P@GNF	5/5		10.30 ± 0.53	0.19 ± 5.91

[a]Weight of P@GNF after being treated with the chloroform/MeOH mixture. [b]Theoretical amount of remaining PCL in P@GNF after being treated with the chloroform/MeOH mixture.

https://dx.doi.org/10.1021/acsomega.0c03902
ACS Omega 2020, 5, 28178−28185

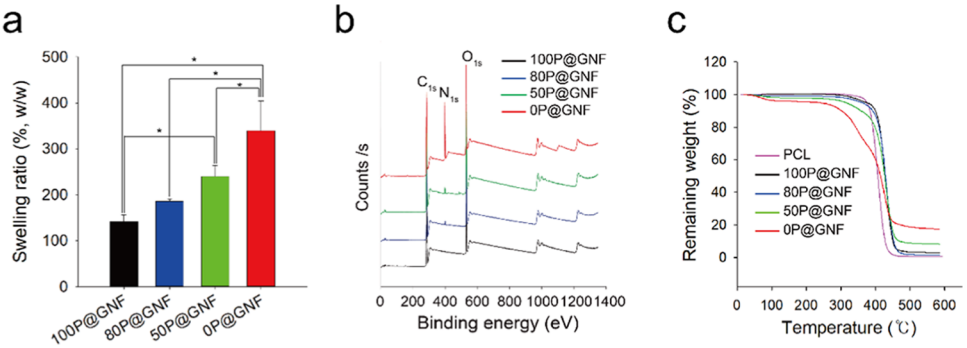

Figure 3. (a) Water swelling ratio of P@G nanofibers with different shell contents (n = 3). (b) XPS spectra of P@G nanofibers with different contents of the PCL shell. (c) Thermogravimetric analysis (TGA) of PCL, 100P@GNF, 80P@GNF, 50P@GNF, and 0P@GNF. (*) shows statistical significance ($p < 0.05$), which was evaluated by one-way analysis of variance (ANOVA).

theoretical weight of the nanofibers collected every 30 min was 0.195 g. Thus, the weight percentages of PCL and gelatin in the nanofibers were calculated to be 88.5 and 11.5%, respectively. Following this, the 100, 80, 50, and 0% PCL remaining in the nanofibrils after treatment with the solvent were theoretically calculated to be 98.23 ± 0.82, 84.00 ± 3.03, 49.71 ± 2.39, and 0.19 ± 5.91%, respectively. By comparing the changes in the weight of P@GNF and the theoretical weight of the remaining PCL, the weight percentage of the remaining PCL after surface etching with chloroform/MeOH (volume ratios of 0/10, 1/9, 3/7, and 5/5) was determined to be approximately 100, 85, 50, and 0% (100P@GNF, 80P@GNF, 50P@GNF, and 0P@GNF), respectively. This result was confirmed by determining the amount of dissolved PCL in the supernatant of the treated solvent (data not shown). These results are consistent with those of our previous study, in which the changes in the weight of the alginate/PCL core–shell nanofibers were measured after completely peeling off the PCL shell.[17]

The characteristics of the P@GNF treated with the chloroform/MeOH mixture (100P@GNF, 80P@GNF, 50P@GNF, and 0P@GNF) are shown in Figure 3. The swelling property of the scaffold is an important concern regarding wound healing and transplantation. Therefore, we first evaluated the swelling ratios of 100P@GNF, 80P@GNF, 50P@GNF, and 0P@GNF (Figure 3a). The swelling ratios of 100P@GNF, 80P@GNF, 50P@GNF, and 0P@GNF were 141.3 ± 15.04, 185.1 ± 5.9, 239.5 ± 24.8, and 339.9 ± 64.9%, respectively. These results indicate that the decrease in the amount of PCL resulted in an increase in the water swelling ratio of P@GNF. Similar behavior was observed in our previous study on the fabrication of alginate-based hydronanofibrous meshes; the water swelling ratio of the remaining alginate (core) nanofibers increased significantly when the PCL shell was completely peeled off.[17] In addition, the water contact angle of the PCL/gelatin composite nanofibers was lower than that of the PCL nanofibers.[32] Therefore, we speculate that the changes in the water swelling ratio of P@GNF are due to the higher exposure of gelatin on the P@GNF surface. To confirm the exposure of gelatin on the surface, the X-ray photoelectron spectroscopy (XPS) spectra of P@GNF were analyzed (Figure 3b). The XPS spectra of all groups clearly exhibited C 1s and O 1s peaks at ∼300 and ∼550 eV, respectively. A distinct peak of N 1s was detected at ∼400 eV in 80P@GNF, 50P@GNF, and gelatin, representing the amine group in gelatin. Although the peak intensity of the XPS spectrum is not quantitative, we confirmed that the peak intensity of N 1s increased gradually as the PCL amount decreased; this indicates that the gelatin at the core was exposed to the surface. A similar XPS spectrum was also observed with a gelatin-derived nitrogen-doped porous carbon in previous works, in which the nitrogen peak appearing at ∼400 eV was attributed to the amino and amide groups in protein.[33] The parameters for the deconvolution of XPS spectra are summarized in Table S1. When the thermal properties of P@GNF were investigated with thermogravimetric analysis (TGA) (Figure 3c), PCL showed a single-stage thermal degradation in the region of 376–460 °C with almost 0% weight remaining. Meanwhile, the 0P@GNF decomposition was recorded in two stages: weight loss from 50 to 220 °C due to the vaporization of moisture and the main thermal degradation zone in the region of 250–600 °C with about 17% weight remaining. In addition, 100P@GNF, 80P@GNF, and 50P@GNF showed a single-stage thermal degradation from 400, 380, and 360 °C, respectively. The remaining weights of 100P@GNF, 80P@GNF, and 50P@GNF at 600 °C were 2.9, 1.5, and 8%, respectively. These results indicate that a smaller PCL amount would result in a greater final remaining weight, and the actual proportions of the PCL remaining in the nanofibrils could be adjusted by varying the volume ratio of chloroform/MeOH in the solvent treatment step. Similar thermal behaviors were also recorded in previous studies with PCL/gelatin composite nanofibers.[32,34]

Viability analysis based on a WST-1 assay was conducted to monitor the proliferation of cells when the NIH3T3 cells were incubated with xP@GNF (Figure 4). On the first day, there were no significant differences between 100P@GNF and 0P@GNF; the cells incubated with 50P@GNF exhibited the highest viability. After 3 days, the proliferation of cells increased rapidly in 80P@GNF, 50P@GNF, and 0P@GNF. The absorbance at 450 nm in these groups was 1.38-, 1.52-, and 3.17-fold higher than that on the first day. By contrast, 100P@GNF exhibited no significant change in cell proliferation. After 5 days, the absorbance of 100P@GNF, 80P@GNF, 50P@GNF, and 0P@GNF increased by 2.40, 1.42, 1.27, and 1.22 times, respectively. On the fifth day, the greatest increase in cell proliferation was observed in the 100P@GNF group, although the absorbance of this group was still significantly lower than that of the other groups. It has been reported that PCL does not facilitate cell adhesion, migration, and proliferation in the long term due to the hydrophobicity of PCL, which results in a lack of wettability.[35] These results suggest that cell proliferation can be enhanced by increasing the exposure of gelatin to the surface of the nanofibrils. It

https://dx.doi.org/10.1021/acsomega.0c03902
ACS Omega 2020, 5, 28178–28185

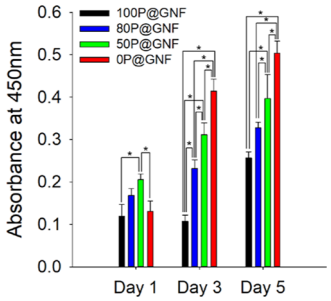

Figure 4. Proliferation of cells cultivated with different shell contents P@GNF for 1, 3, and 5 days (n = 3). NIH3T3 cells were mixed with P@GNF and seeded in a nontreated 48-well plate. WST-1 solution was added to each well and incubated for 1 h at 37 °C, under 5% CO_2 in an incubator in the dark. Supernatant was collected, and the absorbance at 450 nm was measured. (*) shows statistical significance ($p < 0.05$), which was evaluated by one-way ANOVA.

should be noted that although gelatin is widely known as a biocompatible material that supports moisture-rich environments such as hydrogels, surface-immobilized gelatin is expected to play a significant role in the distribution of cell adhesion points for cell cultivation.[36] Several studies have shown that the addition of gelatin to scaffolds enhances the interactions between the cells and the matrix[28,37] but not cell proliferation. We have previously observed a similar degree of cell proliferation between gelatin-immobilized nanofibrils and the PCL nanofibrils when they were cocultured with HaCaT cells and HDF cells to fabricate 3D cell sheets, which suggests that the immobilized gelatin did not have any significant influence on cell proliferation.[22] By contrast, our strategy facilitates 3D cell sheet formation similar to a gelatin-decorated scaffold and enhances cell proliferation similar to a gelatin scaffold.[38]

We cultivated NIH3T3 cells with xP@GNF on nontreated surfaces and monitored the cell spreading by staining the cytoskeleton of NIH3T3 cells (Figure 5a). When cells are cultivated for more than 1 day, they cannot be easily visualized by confocal laser scanning microscopy (CLSM) because the cell numbers are too high. We tried to extend the period up to 5 days; however, cytoskeleton stains for the attached cells were overlapped to a large extent among the stained cells and prevented visualization of individual cells. Thus, we decided to visualize the cytoskeleton after 12 h of cultivation. As a result, the elongation of cells decreased with a decrease in PCL contents. We quantitatively analyzed the CLSM images using ImageJ software to determine the elongation factor of the cells. As shown in Figure 5b, the elongation factors of 100P@GNF, 80P@GNF, 50P@GNF, and 0P@GNF were 3.243 ± 0.49, 2.459 ± 0.405, 2.003 ± 0.26, and 1.878 ± 0.295, respectively. Although there was no significant difference between 50P@GNF and 0P@GNF, a significant difference was observed in the 100P@GNF and 80P@GNF groups when compared to the others. Herein, we supposed that no other control such as cells on tissue culture polystyrene (TCPS) is meaningful in terms of assessing viability because cell culture conditions between two-dimensional (2D) TCPS and 3D cell fibrils are very much different.[39−41] According to the CLSM images and the WST-1 analysis, the cell−matrix interaction in our P@GNF was affected by two factors: (1) different contents of the PCL shell and (2) different exposure of gelatin to culturing environment. At the beginning of cultivation, cell attachment was affected by hydrophobicity of the PCL shell. A previous study determined that the PCL film can adsorb ECM ligands such as collagen I or fibronectin during the cultivation, and then, intergrin receptors of cells can interact with these ligands and adhere onto the scaffold.[24] Moreover, it was confirmed that human mesenchymal stem cells (hMSCs) started to spread on the PCL nanofibrous scaffold after 6−12 h.[25] On the other hand,

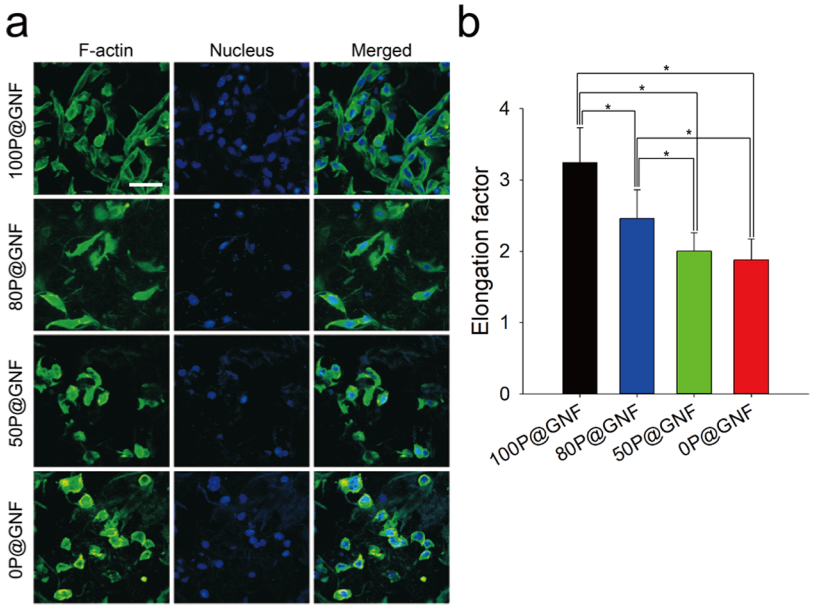

Figure 5. In vitro cultivation of NIH3T3 cells with xP@GNF. (a) Confocal laser scanning microscopy images of NIH3T3 cells with 100P@GNF, 80P@GNF, 50P@GNF, and 0P@GNF cultivated for 12 h and stained with 4′,6-diamidino-2-phenylindole (DAPI) (blue, nucleus) and Alexa Fluor 488 Phalloidin (green, F-actin) (scale bar = 50 μm). (b) Elongation factor was calculated by the following equation: elongation factor = (long axis)/(short axis). Long and short axes were measured by ImageJ (n > 20). (*) shows statistical significance ($p < 0.05$), which was evaluated by one-way ANOVA.

https://dx.doi.org/10.1021/acsomega.0c03902
ACS Omega 2020, 5, 28178−28185

at the later phase of cell proliferation, gelatin plays a vital role in supporting cell proliferation by providing favorable adhesion points and a moisture-rich environment. A previous study demonstrated that cells were seen to elongate and form interconnected networks in GelMA hydrogels after 2 days, which further confirmed our suggested mechanism.[42]

3. CONCLUSIONS

In conclusion, a gelatin-based 3D cell culture support was fabricated by coaxial electrospinning to obtain nanofibers having a core/shell structure with PCL as the shell and gelatin as the core. The gelatin was chemically cross-linked before the nanofibers were fragmented into nanofibrils by physical milling. A controlled surface-etching process with a solvent, where the volume ratio of chloroform/MeOH can be adjusted, was proposed. The validity of the PCL removal method and the exposure of the gelatin core to the surface of the nanofibrils were confirmed using fluorescence microscopy, XPS, and TGA. The cell sheet formation and the spreading behavior of NIH3T3 cells were also investigated. Thus, we envision that *x*P@GNF has the potential to be used in tissue engineering applications due to the enhancement of cell adhesion as well as cell proliferation through the optimized ratio of PCL and gelatin.

4. MATERIALS AND METHODS

4.1. Materials. PCL was purchased from Polysciences (Warminster, PA). Gelatin type A was purchased from MP Biomedicals (Illkirch, France). PVA was purchased from Junsei (Tokyo, Japan). GTA 50% aqueous solution was purchased from Daejung Chemicals & Metals Co., Ltd. (Gyeonggi-do, Republic of Korea). Fluorescein isothiocyanate isomer I (FITC) and 4′,6-diamidino-2-phenylindole (DAPI) dihydrochloride were purchased from Sigma-Aldrich (St. Louis, MO). The formaldehyde solution was purchased from Wako Chemicals (Osaka, Japan). Triton X-100 was purchased from Yakuri Chemicals Co., Ltd. (Tokyo, Japan). Alexa Fluor 488 phalloidin was purchased from Invitrogen (Carlsbad, CA). Dulbecco's modified Eagle's medium (DMEM), phosphate-buffered saline, and streptomycin/penicillin solution were purchased from Gibco (Grand Island, NY). Fetal bovine serum (FBS) was purchased from Capricorn (Ebsdorfergrund, Germany). Mouse embryonic fibroblast cell line NIH3T3 was obtained from the Korean Cell Line Bank (Seoul, Republic of Korea). WST-1 assay solution (EZ Cytox) was purchased from DoGenBio Co., Ltd. (Seoul, Republic of Korea).

4.2. Electrospinning and Cross-linking of P@G Nanofibrous Meshes. P@G nanofibers were fabricated by the coaxial electrospinning of PCL and gelatin type A through a coaxial nozzle. PCL (23%, w/v) was dissolved in chloroform/methanol (3/1, v/v) and incubated overnight at 25−30 °C. Gelatin type A (15%, w/v) and PVA (1%, w/v) were dissolved in distilled water (DW)/acetic acid (9/1, v/v) and incubated overnight at 37 °C. PCL and gelatin/PVA solutions were loaded in 10 and 5 mL syringes, respectively. Both syringes were placed on a syringe pump and pumped at flow rates of 1.5 and 0.3 mL/h, respectively. The applied voltage was 15 kV, and the nanofiber meshes were collected every 30 min on an aluminum foil wrapped around a rotating drum (rotation speed = 200 rpm). The humidity and temperature were adjusted to 25−35% and 20−25 °C, respectively. The collected P@G nanofiber was dried overnight at RT, and the dried P@G nanofiber was detached with 70% ethanol and dried on Kimwipes for 30 min at RT before further cross-linking. To cross-link the gelatin core of P@G nanofibers, the nanofibrous meshes were immersed in GTA solution (GTA/DW/ethanol = 5/47.5/47.5, v/v/v) for 2 h on a 2D shaker at 125 rpm (GTA solution/nanofibrous meshes = 100/1, v/w). Then, the nanofibrous meshes were washed three times with ethanol and dried using Kimwipes for 30 min at 25−30 °C.

4.3. Preparation of *x*P@GNF. To prepare 100P@GNF, which was with 100% remaining PCL on the surface of nanofibrils, the cross-linked P@G nanofibers were milled 10 times (for 30 s each time) using an analytical mill and immersed in an ethanol/DW (5/5, v/v) solution. The ethanol/DW (5/5, v/v) solution with P@G nanofibrils (P@GNF) was filtered three times through a sieve having a pore size of 160 μm. The P@GNF was collected through centrifugation at 3000 rpm for 10 min, washed with ethanol (twice) and DW (three times), and then freeze-dried.

To prepare 80P@GNF, 50P@GNF, and 0P@GNF having 80, 50, and 0% remaining PCL, accordingly, cross-linked P@G nanofibers were milled 10 times (for 30 s each time) using an analytical mill and immersed in an ethanol/DW (5/5, v/v) solution. The ethanol/DW (5/5, v/v) solution with P@GNF was filtered through a sieve having a pore size of 160 μm. Afterward, the filtered nanofibrils were collected and washed three times each with ethanol and DW and then freeze-dried. Completely lyophilized nanofibrils were weighed and placed in a round-bottom flask with a magnetic bar. For the solvent treatment, the solvent mixture was prepared with a 2/1 (mg/mL) ratio of nanofibrils to the chloroform/methanol mixture. First, the nanofibrils were homogeneously mixed with methanol in a round-bottom flask and stirred for 10 min using a magnetic bar. Then, chloroform was slowly dropped into the round-bottom flask through a 10 mL syringe at a flow rate of 18 mL/h. The final volume ratio of chloroform/methanol was 1/9, 3/7, and 5/5 to obtain 80P@GNF, 50P@GNF, and 0P@GNF, respectively. After adding chloroform, incubation was performed with continuous stirring at RT for 1 h. After 1 h, methanol was added to the round-bottom flask (volume ratio of methanol and chloroform/methanol was 1/1) and incubated for 10 min at RT. The treated nanofibrils were collected through centrifugation at 3000 rpm for 10 min and washed with ethanol three times. The ethanol was discarded, and the collected nanofibrils were vacuum-dried overnight. The dried nanofibrils were weighed to measure the PCL loss and milled 10 times (for 30 s each time) using an analytical mill and immersed in an ethanol/DW (5/5, v/v) solution. The ethanol/DW (5/5, v/v) solution with P@GNF was filtered through a sieve having a pore size of 160 μm. The 80P@GNF and 50P@GNF were collected through centrifugation at 3000 rpm for 10 min, washed with ethanol (twice) and DW (three times), and then freeze-dried.

4.4. Measurement of Exposed Gelatin on the Surface. To measure the amount of exposed gelatin core on the surface, FITC-labeled gelatin was prepared. Briefly, gelatin type A was dissolved in 0.1 M sodium carbonate buffer (pH = 9, 50 mg/mL) and FITC was predissolved in dimethyl sulfoxide (DMSO) (1 mg/mL) before being added to the gelatin solution with a volume ratio of FITC/gelatin of 1/20. The reaction was performed at 37 °C in dark conditions with gentle stirring for 8 h; FITC-labeled gelatin was collected by precipitation in ethanol and further washed with ethanol (three times) before being vacuum-dried. Then, the P@FITC-

https://dx.doi.org/10.1021/acsomega.0c03902
ACS Omega 2020, 5, 28178−28185

labeled gelatin nanofiber was treated with chloroform/methanol. P@FITC-labeled gelatin nanofiber was fabricated using a coaxial nozzle. The P@FITC-labeled gelatin nanofiber was treated with 0, 10, and 30% chloroform in methanol with respect to obtain 100P@GNF, 80P@GNF, and 50P@GNF and subsequently washed with ethanol three times prior to observation under a fluorescence microscope.

4.5. Swelling Ratio. The swelling ratio of the solvent mixture-treated P@GNF was detected by measuring the weight of the P@GNF before and after swelling. The solvent mixture-treated P@GNF was soaked in DW at 37 °C for 50 min. After 50 min, the excess water on the surface was removed using Kimwipes for 20 s and the weight was measured. The swelling ratio of the P@GNF (n = 3) was gravimetrically determined using the following formula: swelling ratio (%) = $(W_s/W_d) \times 100$ (%), where W_d is the weight of the dried P@GNF and W_s is the weight of the swollen P@GNF.

4.6. Characterization of *x*P@GNF. To observe the morphology of the *x*P@GNF, it was dispersed in ethanol and placed on an aluminum foil prior to observation using an ultra-high-resolution scanning electron microscope (UHR-SEM) (S-4800; HITACHI, Japan) at the Central Laboratory of Kangwon National University. The exposed gelatin on the surface was confirmed through X-ray photoelectron spectroscopy (XPS) (K Alpha+; Thermo Scientific, U.K.) at the Central Laboratory of Kangwon National University, and survey scans of C 1s, O 1s, and N 1s were obtained. The thermal degradation behaviors of *x*P@GNF were measured using a thermogravimetric analyzer (SDT Q600; TA Instruments). The temperature was increased from 25 to 600 °C at a heating rate of 10 °C/min under a nitrogen atmosphere at the Central Laboratory of Kangwon National University.

4.7. Fabrication of *x*P@GNF/Cell Sheets. A suspension of NIH3T3 cells (0.4 mL, 2 × 10^5 cells/well) in DMEM supplemented with 10% (v/v) FBS and 1% (v/v) streptomycin/penicillin was homogeneously mixed with 100P@GNF, 80P@GNF, 50P@GNF, and 0P@GNF (2 mg, n = 3) by gentle pipetting, and the mixture was seeded on a nontreated 48-well plate. The matrix/cell complexes were cultured at 37 °C under 5% CO_2. The cell culture medium was replaced with fresh DMEM daily. After 1, 3, and 5 days, the cell proliferation was determined by a WST-1 based colorimetric assay, according to the manufacturer's protocol. The entire medium in the nontreated 48-well plate was discarded, and 200 μL of the medium was added. Then, 20 μL of WST-1 solution was added to each well and incubated at 37 °C under 5% CO_2 for 1 h. The absorbance of the medium was measured at 450 nm (Multiscam GO; Thermo Scientific, U.K.). To evaluate the effect of 100P@GNF, 80P@GNF, 50P@GNF, and 0P@GNF on cell proliferation and spreading, the *x*P@GNF/cell complexes were fixed with 3.7% formaldehyde for 50 min and then with 0.5% (v/v) Triton X-100 for 5 min. The cytoskeleton and nucleus in the *x*P@GNF/cell complexes were stained with Alexa Fluor 488 phalloidin for 50 min and counterstained with DAPI for 1 min. The *x*P@GNF/cell complexes were visualized by confocal laser scanning microscopy (CLSM) (LSM880; Carl Zeiss, Germany) using a diode laser at 405 nm and a Mar laser at 488 nm for DAPI and Alexa Fluor 488 phalloidin, respectively, at the Central Laboratory of Kangwon National University. In addition, we evaluated the elongation factor of individual cells by analyzing the CLSM images. The elongation factor was calculated by dividing the long axis by the short axis as follows:

$$\text{Elongation factor} = (\text{Long axis}/\text{short axis})$$

■ ASSOCIATED CONTENT

Supporting Information

The Supporting Information is available free of charge at https://pubs.acs.org/doi/10.1021/acsomega.0c03902.

Characterization of P@G nanofiber with different flow rates of PCL (PDF)

■ AUTHOR INFORMATION

Corresponding Author

Hyuk Sang Yoo − *Department of Biomedical Materials Engineering and Institute of Bioscience and Biotechnology, Kangwon National University, Chuncheon 24341, Republic of Korea;* orcid.org/0000-0002-4346-9154; Email: hsyoo@kangwon.ac.kr; http://nano-bio.kangwon.ac.kr

Authors

Jae Keun Park − *Department of Biomedical Materials Engineering, Kangwon National University, Chuncheon 24341, Republic of Korea*

Oanh-Vu Pham-Nguyen − *Department of Biomedical Materials Engineering, Kangwon National University, Chuncheon 24341, Republic of Korea*

Complete contact information is available at: https://pubs.acs.org/10.1021/acsomega.0c03902

Author Contributions

§J.K.P. and O.-V.P.-N. contributed equally to this work.

Notes

The authors declare no competing financial interest.

■ ACKNOWLEDGMENTS

This work was supported by the Ministry of Education and the Ministry of Science and ICT in Republic of Korea (2019R1I1A2A01040849; 2020R1A4A1016093). We also appreciate Chuncheon branch of the Korea Basic Science Institute for the financial support.

■ REFERENCES

(1) Chen, W.; Ma, J.; Zhu, L.; Morsi, Y.; EI-Hamshary, H.; Al-Deyab, S. S.; Mo, X. Superelastic, Superabsorbent and 3D Nanofiber-Assembled Scaffold for Tissue Engineering. *Colloids Surf., B* **2016**, *142*, 165−172.

(2) Holzwarth, J. M.; Ma, P. X. Biomimetic Nanofibrous Scaffolds for Bone Tissue Engineering. *Biomaterials* **2011**, *32*, 9622−9629.

(3) Kadler, K. Matrix Loading: Assembly of Extracellular Matrix Collagen Fibrils during Embryogenesis. *Birth Defects Res., Part C* **2004**, *72*, 1−11.

(4) Lee, S.; Kim, H. S.; Yoo, H. S. Electrospun Nanofibrils Embedded Hydrogel Composites for Cell Cultivation in a Biomimetic Environment. *RSC Adv.* **2017**, *7*, 54246−54253.

(5) Antoni, D.; Burckel, H.; Josset, E.; Noel, G. Three-Dimensional Cell Culture: A Breakthrough in Vivo. *Int. J. Mol. Sci.* **2015**, *16*, 5517−5527.

(6) Yang, Y.; Basu, S.; Tomasko, D. L.; Lee, L. J.; Yang, S. T. Fabrication of Well-Defined PLGA Scaffolds Using Novel Micro-embossing and Carbon Dioxide Bonding. *Biomaterials* **2005**, *26*, 2585−2594.

(7) Billiet, T.; Gevaert, E.; De Schryver, T.; Cornelissen, M.; Dubruel, P. The 3D Printing of Gelatin Methacrylamide Cell-Laden

Tissue-Engineered Constructs with High Cell Viability. *Biomaterials* **2014**, *35*, 49−62.
(8) Shin, S. H.; Purevdorj, O.; Castano, O.; Planell, J. A.; Kim, H. W. A Short Review: Recent Advances in Electrospinning for Bone Tissue Regeneration. *J. Tissue Eng.* **2012**, *3*, 1−11.
(9) Yu, D. G.; Branford-White, C.; Bligh, S. W. A.; White, K.; Chatterton, N. P.; Zhu, L. M. Improving Polymer Nanofiber Quality Using a Modified Co-Axial Electrospinning Process. *Macromol. Rapid Commun.* **2011**, *32*, 744−750.
(10) Park, B. U.; Park, S. M.; Lee, K. P.; Lee, S. J.; Nam, Y. E.; Park, H. S.; Eom, S.; Lim, J. O.; Kim, D. S.; Kim, H. K. Collagen Immobilization on Ultra-Thin Nanofiber Membrane to Promote in Vitro Endothelial Monolayer Formation. *J. Tissue Eng.* **2019**, *10*, 1−12.
(11) Liu, M.; Duan, X. P.; Li, Y. M.; Yang, D. P.; Long, Y. Z. Electrospun Nanofibers for Wound Healing. *Mater. Sci. Eng., C* **2017**, *76*, 1413−1423.
(12) Bhardwaj, N.; Kundu, S. C. Electrospinning: A Fascinating Fiber Fabrication Technique. *Biotechnol. Adv.* **2010**, *28*, 325−347.
(13) Li, W. J.; Tuli, R.; Okafor, C.; Derfoul, A.; Danielson, K. G.; Hall, D. J.; Tuan, R. S. A Three-Dimensional Nanofibrous Scaffold for Cartilage Tissue Engineering Using Human Mesenchymal Stem Cells. *Biomaterials* **2005**, *26*, 599−609.
(14) Nisbet, D. R.; Rodda, A. E.; Horne, M. K.; Forsythe, J. S.; Finkelstein, D. I. Neurite Infiltration and Cellular Response to Electrospun Polycaprolactone Scaffolds Implanted into the Brain. *Biomaterials* **2009**, *30*, 4573−4580.
(15) Kim, M. S.; Jun, I.; Shin, Y. M.; Jang, W.; Kim, S. I.; Shin, H. The Development of Genipin-Crosslinked Poly(Caprolactone) (PCL)/Gelatin Nanofibers for Tissue Engineering Applications. *Macromol. Biosci.* **2010**, *10*, 91−100.
(16) Lee, B. K.; Ju, Y. M.; Cho, J. G.; Jackson, J. D.; Lee, S. J.; Atala, A.; Yoo, J. J. End-to-Side Neurorrhaphy Using an Electrospun PCL/Collagen Nerve Conduit for Complex Peripheral Motor Nerve Regeneration. *Biomaterials* **2012**, *33*, 9027−9036.
(17) Son, Y. J.; Kim, H. S.; Mao, W.; Park, J. B.; Lee, D.; Lee, H.; Yoo, H. S. Hydro-Nanofibrous Mesh Deep Cell Penetration: A Strategy Based on Peeling of Electrospun Coaxial Nanofibers. *Nanoscale* **2018**, *10*, 6051−6059.
(18) Pham-Nguyen, O.-V.; Shin, J. U.; Kim, H.; Yoo, H. S. Self-Assembled Cell Sheets Composed of Mesenchymal Stem Cell and Gelatin Nanofiber for Treatment of Full Thickness Wounds. *Biomater. Sci.* **2020**, *8*, 4535−4544.
(19) Son, Y. J.; Tse, J. W.; Zhou, Y.; Mao, W.; Yim, E. K. F.; Yoo, H. S. Biomaterials and Controlled Release Strategy for Epithelial Wound Healing. *Biomater. Sci.* **2019**, *7*, 4444−4471.
(20) Kim, H. S.; Mandakhbayar, N.; Kim, H. W.; Leong, K. W.; Yoo, H. S. Protein-Reactive Nanofibrils Decorated with Cartilage-Derived Decellularized Extracellular Matrix for Osteochondral Defects. *Biomaterials* **2020**, No. 120214.
(21) Lee, J. W.; Yoo, H. S. Michael-Type Addition of Gelatin on Electrospun Nanofibrils for Self-Assembly of Cell Sheets Composed of Human Dermal Fibroblasts. *ACS Omega* **2019**, *4*, 18677−18684.
(22) Mao, W.; Kang, M. K.; Shin, J. U.; Son, Y. J.; Kim, H. S.; Yoo, H. S. Coaxial Hydro-Nanofibrils for Self-Assembly of Cell Sheets Producing Skin Bilayers. *ACS Appl. Mater. Interfaces* **2018**, *10*, 43503−43511.
(23) Mao, W.; Lee, S.; Kim, S. R.; Kim, K. N.; Yoo, H. S. Electrospun Nanohybrid Hydrogels for Enhanced Differentiation of Myoblasts. *J. Ind. Eng. Chem.* **2019**, *80*, 838−845.
(24) Li, M.; Mondrinos, M. J.; Chen, X.; Gandhi, M. R.; Ko, F. K.; Lelkes, P. I. Co-electrospun poly(lactide-co-glycolide), gelatin, and elastin blends for tissue engineering scaffolds. *J. Biomed. Mater. Res., Part A* **2006**, *79A*, 963−973.
(25) Binulal, N. S.; Deepthy, M.; Selvamurugan, N.; Shalumon, K. T.; Suja, S.; Mony, U.; Jayakumar, R.; Nair, S. V. Role of Nanofibrous Poly(Caprolactone) Scaffolds in Human Mesenchymal Stem Cell Attachment and Spreading for in Vitro Bone Tissue Engineering-Response to Osteogenic Regulators. *Tissue Eng., Part A* **2010**, *16*, 393−404.
(26) Huang, Z. M.; Zhang, Y. Z.; Ramakrishna, S.; Lim, C. T. Electrospinning and Mechanical Characterization of Gelatin Nanofibers. *Polymer* **2004**, *45*, 5361−5368.
(27) Rho, K. S.; Jeong, L.; Lee, G.; Seo, B. M.; Park, Y. J.; Hong, S. D.; Roh, S.; Cho, J. J.; Park, W. H.; Min, B. M. Electrospinning of Collagen Nanofibers: Effects on the Behavior of Normal Human Keratinocytes and Early-Stage Wound Healing. *Biomaterials* **2006**, *27*, 1452−1461.
(28) Sarker, B.; Singh, R.; Silva, R.; Roether, J. A.; Kaschta, J.; Detsch, R.; Schubert, D. W.; Cicha, I.; Boccaccini, A. R. Evaluation of Fibroblasts Adhesion and Proliferation on Alginate-Gelatin Cross-linked Hydrogel. *PLoS One* **2014**, *9*, No. e107952.
(29) Kim, H. S.; Yoo, H. S. Surface-Polymerized Biomimetic Nanofibrils for the Cell-Directed Association of 3-D Scaffolds. *Chem. Commun.* **2015**, *51*, 306−309.
(30) Son, Y. J.; Kim, H. S.; Choi, D. H.; Yoo, H. S. Multilayered Electrospun Fibrous Meshes for Restenosis-Suppressing Metallic Stents. *J. Biomed. Mater. Res., Part B* **2017**, *105*, 628−635.
(31) Zhang, Y.; Ouyang, H.; Chwee, T. L.; Ramakrishna, S.; Huang, Z. M. Electrospinning of Gelatin Fibers and Gelatin/PCL Composite Fibrous Scaffolds. *J. Biomed. Mater. Res., Part B* **2005**, *72B*, 156−165.
(32) Ren, K.; Wang, Y.; Sun, T.; Yue, W.; Zhang, H. Electrospun PCL/Gelatin Composite Nanofiber Structures for Effective Guided Bone Regeneration Membranes. *Mater. Sci. Eng., C* **2017**, *78*, 324−332.
(33) Chen, X. Y.; Chen, C.; Zhang, Z. J.; Xie, D. H. Gelatin-Derived Nitrogen-Doped Porous Carbon via a Dual-Template Carbonization Method for High Performance Supercapacitors. *J. Mater. Chem. A* **2013**, *1*, 10903−10911.
(34) Gautam, S.; Dinda, A. K.; Mishra, N. C. Fabrication and Characterization of PCL/Gelatin Composite Nanofibrous Scaffold for Tissue Engineering Applications by Electrospinning Method. *Mater. Sci. Eng., C* **2013**, *33*, 1228−1235.
(35) Cipitria, A.; Skelton, A.; Dargaville, T. R.; Dalton, P. D.; Hutmacher, D. W. Design, Fabrication and Characterization of PCL Electrospun Scaffolds - A Review. *J. Mater. Chem.* **2011**, *21*, 9419−9453.
(36) Kim, J. I.; Kim, C. S. Harnessing Nanotopography of PCL/Collagen Nanocomposite Membrane and Changes in Cell Morphology Coordinated with Wound Healing Activity. *Mater. Sci. Eng., C* **2018**, *91*, 824−837.
(37) Meghdadi, M.; Atyabi, S.-M.; Pezeshki-Modaress, M.; Irani, S.; Noormohammadi, Z.; Zandi, M. Cold Atmospheric Plasma as a Promising Approach for Gelatin Immobilization on Poly(ε-Caprolactone) Electrospun Scaffolds. *Prog. Biomater.* **2019**, *8*, 65−75.
(38) Sisson, K.; Zhang, C.; Farach-Carson, M. C.; Chase, D. B.; Rabolt, J. F. Evaluation of Cross-Linking Methods for Electrospun Gelatin on Cell Growth and Viability. *Biomacromolecules* **2009**, *10*, 1675−1680.
(39) Fleischer, S.; Jahnke, H. G.; Fritsche, E.; Girard, M.; Robitzki, A. A. Comprehensive Human Stem Cell Differentiation in a 2D and 3D Mode to Cardiomyocytes for Long-Term Cultivation and Multiparametric Monitoring on a Multimodal Microelectrode Array Setup. *Biosens. Bioelectron.* **2019**, *126*, 624−631.
(40) Luca, A. C.; Mersch, S.; Deenen, R.; Schmidt, S.; Messner, I.; Schäfer, K. L.; Baldus, S. E.; Huckenbeck, W.; Piekorz, R. P.; Knoefel, W. T.; Krieg, A.; Stoecklein, N. H. Impact of the 3D Microenvironment on Phenotype, Gene Expression, and EGFR Inhibition of Colorectal Cancer Cell Lines. *PLoS One* **2013**, *8*, No. e59689.
(41) Schyschka, L.; Sánchez, J. J. M.; Wang, Z.; Burkhardt, B.; Müller-Vieira, U.; Zeilinger, K.; Bachmann, A.; Nadalin, S.; Damm, G.; Nussler, A. K. Hepatic 3D Cultures but Not 2D Cultures Preserve Specific Transporter Activity for Acetaminophen-Induced Hepatotoxicity. *Arch. Toxicol.* **2013**, *87*, 1581−1593.
(42) Nichol, J. W.; Koshy, S. T.; Bae, H.; Hwang, C. M.; Yamanlar, S.; Khademhosseini, A. Cell-Laden Microengineered Gelatin Methacrylate Hydrogels. *Biomaterials* **2010**, *31*, 5536−5544.

https://dx.doi.org/10.1021/acsomega.0c03902
ACS Omega 2020, 5, 28178−28185